Centrality-Dependent Modification of Jet-Production Rates in Deuteron-Gold Collisions at √sNN=200 GeV

(PHENIX Collaboration) Adare, A.; ...; Makek, Mihael; ...; Zou, L.

Journal article, Published version
Rad u časopisu, Objavljena verzija rada (izdavačev PDF)

Permanent link / Trajna poveznica: https://urn.nsk.hr/urn:nbn:hr:217:297397

Download date / Datum preuzimanja: **2024-08-06**

Centrality-Dependent Modification of Jet-Production Rates in Deuteron-Gold Collisions at $\sqrt{s_{NN}} = 200$ GeV

A. Adare,[13] C. Aidala,[43,44] N. N. Ajitanand,[64] Y. Akiba,[58,59] H. Al-Bataineh,[52] J. Alexander,[64] M. Alfred,[23] A. Angerami,[14] K. Aoki,[32,35,58] N. Apadula,[28,65] Y. Aramaki,[12,58] H. Asano,[35,58] E. T. Atomssa,[36] R. Averbeck,[65] T. C. Awes,[54] B. Azmoun,[7] V. Babintsev,[24] M. Bai,[6] G. Baksay,[19] L. Baksay,[19] N. S. Bandara,[43] B. Bannier,[65] K. N. Barish,[8] B. Bassalleck,[51] A. T. Basye,[1] S. Bathe,[5,8,59] V. Baublis,[57] C. Baumann,[7,45] A. Bazilevsky,[7] M. Beaumier,[8] S. Beckman,[13] S. Belikov,[7,*] R. Belmont,[13,44,69] R. Bennett,[65] A. Berdnikov,[61] Y. Berdnikov,[61] J. H. Bhom,[73] D. S. Blau,[34] J. S. Bok,[52,73] K. Boyle,[59,65] M. L. Brooks,[39] J. Bryslawskyj,[5] H. Buesching,[7] V. Bumazhnov,[24] G. Bunce,[7,59] S. Butsyk,[39] S. Campbell,[14,28,65] A. Caringi,[46] C.-H. Chen,[59,65] C. Y. Chi,[14] M. Chiu,[7] I. J. Choi,[25,73] J. B. Choi,[10] R. K. Choudhury,[4] P. Christiansen,[41] T. Chujo,[68] P. Chung,[64] O. Chvala,[8] V. Cianciolo,[54] Z. Citron,[65,71] B. A. Cole,[14] Z. Conesa del Valle,[36] M. Connors,[65] M. Csanád,[17] T. Csörgő,[72] T. Dahms,[65] S. Dairaku,[35,58] I. Danchev,[69] T. W. Danley,[53] K. Das,[20] A. Datta,[43,51] M. S. Daugherity,[1] G. David,[7] M. K. Dayananda,[21] K. DeBlasio,[51] K. Dehmelt,[65] A. Denisov,[24] A. Deshpande,[59,65] E. J. Desmond,[7] K. V. Dharmawardane,[52] O. Dietzsch,[62] A. Dion,[28,65] P. B. Diss,[42] J. H. Do,[73] M. Donadelli,[62] L. D'Orazio,[42] O. Drapier,[36] A. Drees,[65] K. A. Drees,[6] J. M. Durham,[39,65] A. Durum,[24] D. Dutta,[4] S. Edwards,[20] Y. V. Efremenko,[54] F. Ellinghaus,[13] T. Engelmore,[14] A. Enokizono,[54,58,60] H. En'yo,[58,59] S. Esumi,[68] B. Fadem,[46] N. Feege,[65] D. E. Fields,[51] M. Finger,[9] M. Finger, Jr.,[9] F. Fleuret,[36] S. L. Fokin,[34] Z. Fraenkel,[71,*] J. E. Frantz,[53,65] A. Franz,[7] A. D. Frawley,[20] K. Fujiwara,[58] Y. Fukao,[58] T. Fusayasu,[48] C. Gal,[65] P. Gallus,[15] P. Garg,[3] I. Garishvili,[38,66] H. Ge,[65] F. Giordano,[25] A. Glenn,[38] H. Gong,[65] M. Gonin,[36] Y. Goto,[58,59] R. Granier de Cassagnac,[36] N. Grau,[2,14] S. V. Greene,[69] G. Grim,[39] M. Grosse Perdekamp,[25] T. Gunji,[12] H.-Å. Gustafsson,[41,*] T. Hachiya,[58] J. S. Haggerty,[7] K. I. Hahn,[18] H. Hamagaki,[12] J. Hamblen,[66] H. F. Hamilton,[1] R. Han,[56] S. Y. Han,[18] J. Hanks,[14,65] S. Hasegawa,[29] T. O. S. Haseler,[21] K. Hashimoto,[58,60] E. Haslum,[41] R. Hayano,[12] X. He,[21] M. Heffner,[38] T. K. Hemmick,[65] T. Hester,[8] J. C. Hill,[28] M. Hohlmann,[19] R. S. Hollis,[8] W. Holzmann,[14] K. Homma,[22] B. Hong,[33] T. Horaguchi,[22] D. Hornback,[66] T. Hoshino,[22] N. Hotvedt,[28] J. Huang,[7] S. Huang,[69] T. Ichihara,[58,59] R. Ichimiya,[58] Y. Ikeda,[68] K. Imai,[29,35,58] M. Inaba,[68] A. Iordanova,[8] D. Isenhower,[1] M. Ishihara,[58] M. Issah,[69] D. Ivanishchev,[57] Y. Iwanaga,[22] B. V. Jacak,[65] M. Jezghani,[21] J. Jia,[7,64] X. Jiang,[39] J. Jin,[14] B. M. Johnson,[7] T. Jones,[1] K. S. Joo,[47] D. Jouan,[55] D. S. Jumper,[1,25] F. Kajihara,[12] J. Kamin,[65] S. Kanda,[12] J. H. Kang,[73] J. Kapustinsky,[39] K. Karatsu,[35,58] M. Kasai,[58,60] D. Kawall,[43,59] M. Kawashima,[58,60] A. V. Kazantsev,[34] T. Kempel,[28] J. A. Key,[51] V. Khachatryan,[65] A. Khanzadeev,[57] K. M. Kijima,[22] J. Kikuchi,[70] A. Kim,[18] B. I. Kim,[33] C. Kim,[33] D. J. Kim,[30] E.-J. Kim,[10] G. W. Kim,[18] M. Kim,[63] Y.-J. Kim,[25] B. Kimelman,[46] E. Kinney,[13] Á. Kiss,[17] E. Kistenev,[7] R. Kitamura,[12] J. Klatsky,[20] D. Kleinjan,[8] P. Kline,[65] T. Koblesky,[13] L. Kochenda,[57] B. Komkov,[57] M. Konno,[68] J. Koster,[25] D. Kotov,[57,61] A. Král,[15] A. Kravitz,[14] G. J. Kunde,[39] K. Kurita,[58,60] M. Kurosawa,[58,59] Y. Kwon,[73] G. S. Kyle,[52] R. Lacey,[64] Y. S. Lai,[14] J. G. Lajoie,[28] D. M. Lee,[39] J. Lee,[18] K. B. Lee,[33] K. S. Lee,[33] S. Lee,[73] S. H. Lee,[65] M. J. Leitch,[39] M. A. L. Leite,[62] X. Li,[11] P. Lichtenwalner,[46] P. Liebing,[59] S. H. Lim,[73] L. A. Linden Levy,[13] T. Liška,[15] H. Liu,[39] M. X. Liu,[39] B. Love,[69] D. Lynch,[7] C. F. Maguire,[69] Y. I. Makdisi,[6] M. Makek,[74] M. D. Malik,[51] A. Manion,[65] V. I. Manko,[34] E. Mannel,[7,14] Y. Mao,[56,58] H. Masui,[68] F. Matathias,[14] M. McCumber,[39,65] P. L. McGaughey,[39] D. McGlinchey,[13,20] C. McKinney,[25] N. Means,[65] A. Meles,[52] M. Mendoza,[8] B. Meredith,[25] Y. Miake,[68] T. Mibe,[32] A. C. Mignerey,[42] K. Miki,[58,68] A. Milov,[7,71] D. K. Mishra,[4] J. T. Mitchell,[7] S. Miyasaka,[58,67] S. Mizuno,[58,68] A. K. Mohanty,[4] P. Montuenga,[25] H. J. Moon,[47] T. Moon,[73] Y. Morino,[12] A. Morreale,[8] D. P. Morrison,[7,†] T. V. Moukhanova,[34] T. Murakami,[35,58] J. Murata,[58,60] A. Mwai,[64] S. Nagamiya,[32,58] K. Nagashima,[22] J. L. Nagle,[13,‡] M. Naglis,[71] M. I. Nagy,[17,72] I. Nakagawa,[58,59] H. Nakagomi,[58,68] Y. Nakamiya,[22] K. R. Nakamura,[35,58] T. Nakamura,[58] K. Nakano,[58,67] S. Nam,[18] C. Nattrass,[66] P. K. Netrakanti,[4] J. Newby,[38] M. Nguyen,[65] M. Nihashi,[22] T. Niida,[68] S. Nishimura,[12] R. Nouicer,[7,59] T. Novák,[31,72] N. Novitzky,[30,65] A. S. Nyanin,[34] C. Oakley,[21] E. O'Brien,[7] S. X. Oda,[12] C. A. Ogilvie,[28] M. Oka,[68] K. Okada,[59] Y. Onuki,[58] J. D. Orjuela Koop,[13] J. D. Osborn,[44] A. Oskarsson,[41] M. Ouchida,[22,58] K. Ozawa,[12,32] R. Pak,[7] V. Pantuev,[26,65] V. Papavassiliou,[52] I. H. Park,[18] J. S. Park,[63] S. Park,[63] S. K. Park,[33] W. J. Park,[33] S. F. Pate,[52] M. Patel,[28] H. Pei,[28] J.-C. Peng,[25] H. Pereira,[16] D. V. Perepelitsa,[7] G. D. N. Perera,[52] D. Yu. Peressounko,[34] J. Perry,[28] R. Petti,[7,65] C. Pinkenburg,[7] R. Pinson,[1] R. P. Pisani,[7] M. Proissl,[65] M. L. Purschke,[7] H. Qu,[21] J. Rak,[30] B. J. Ramson,[44] I. Ravinovich,[71] K. F. Read,[54,66] S. Rembeczki,[19] K. Reygers,[45] D. Reynolds,[64] V. Riabov,[50,57] Y. Riabov,[57,61] E. Richardson,[42] T. Rinn,[28] D. Roach,[69] G. Roche,[40,*] S. D. Rolnick,[8] M. Rosati,[28] C. A. Rosen,[13] S. S. E. Rosendahl,[41] Z. Rowan,[5] J. G. Rubin,[44] P. Ružička,[27] B. Sahlmueller,[45,65] N. Saito,[32] T. Sakaguchi,[7] K. Sakashita,[58,67] H. Sako,[29] V. Samsonov,[50,57] S. Sano,[12,70] M. Sarsour,[21] S. Sato,[29,32] T. Sato,[68] S. Sawada,[32] B. Schaefer,[69]

B. K. Schmoll,[66] K. Sedgwick,[8] J. Seele,[13] R. Seidl,[25,58,59] A. Sen,[66] R. Seto,[8] P. Sett,[4] A. Sexton,[42] D. Sharma,[65,71] I. Shein,[24] T.-A. Shibata,[58,67] K. Shigaki,[22] M. Shimomura,[28,49,68] K. Shoji,[35,58] P. Shukla,[4] A. Sickles,[7,25] C. L. Silva,[28,39] D. Silvermyr,[41,54] C. Silvestre,[16] K. S. Sim,[33] B. K. Singh,[3] C. P. Singh,[3] V. Singh,[3] M. Slunečka,[9] M. Snowball,[39] R. A. Soltz,[38] W. E. Sondheim,[39] S. P. Sorensen,[66] I. V. Sourikova,[7] P. W. Stankus,[54] E. Stenlund,[41] M. Stepanov,[43,52,*] S. P. Stoll,[7] T. Sugitate,[22] A. Sukhanov,[7] T. Sumita,[58] J. Sun,[65] J. Sziklai,[72] E. M. Takagui,[62] A. Taketani,[58,59] R. Tanabe,[68] Y. Tanaka,[48] S. Taneja,[65] K. Tanida,[35,58,59,63] M. J. Tannenbaum,[7] S. Tarafdar,[3,71] A. Taranenko,[50,64] H. Themann,[65] D. Thomas,[1] T. L. Thomas,[51] R. Tieulent,[21] A. Timilsina,[28] T. Todoroki,[58,68] M. Togawa,[59] A. Toia,[65] L. Tomášek,[27] M. Tomášek,[15,27] H. Torii,[22] C. L. Towell,[1] R. Towell,[1] R. S. Towell,[1] I. Tserruya,[71] Y. Tsuchimoto,[22] C. Vale,[7] H. Valle,[69] H. W. van Hecke,[39] E. Vazquez-Zambrano,[14] A. Veicht,[14,25] J. Velkovska,[69] R. Vértesi,[72] M. Virius,[15] V. Vrba,[15,27] E. Vznuzdaev,[57] X. R. Wang,[52,59] D. Watanabe,[22] K. Watanabe,[68] Y. Watanabe,[58,59] Y. S. Watanabe,[12,32] F. Wei,[28,52] R. Wei,[64] J. Wessels,[45] A. S. White,[44] S. N. White,[7] D. Winter,[14] C. L. Woody,[7] R. M. Wright,[1] M. Wysocki,[13,54] B. Xia,[53] L. Xue,[21] S. Yalcin,[65] Y. L. Yamaguchi,[12,58,65] K. Yamaura,[22] R. Yang,[25] A. Yanovich,[24] J. Ying,[21] S. Yokkaichi,[58,59] J. H. Yoo,[33] I. Yoon,[63] Z. You,[56] G. R. Young,[54] I. Younus,[37,51] H. Yu,[56] I. E. Yushmanov,[34] W. A. Zajc,[14] A. Zelenski,[6] S. Zhou,[11] and L. Zou[8]

(PHENIX Collaboration)

[1]*Abilene Christian University, Abilene, Texas 79699, USA*
[2]*Department of Physics, Augustana University, Sioux Falls, South Dakota 57197, USA*
[3]*Department of Physics, Banaras Hindu University, Varanasi 221005, India*
[4]*Bhabha Atomic Research Centre, Bombay 400 085, India*
[5]*Baruch College, City University of New York, New York, New York 10010, USA*
[6]*Collider-Accelerator Department, Brookhaven National Laboratory, Upton, New York 11973-5000, USA*
[7]*Physics Department, Brookhaven National Laboratory, Upton, New York 11973-5000, USA*
[8]*University of California-Riverside, Riverside, California 92521, USA*
[9]*Charles University, Ovocný trh 5, Praha 1, 116 36, Prague, Czech Republic*
[10]*Chonbuk National University, Jeonju, 561-756, Korea*
[11]*Science and Technology on Nuclear Data Laboratory, China Institute of Atomic Energy, Beijing 102413, People's Republic of China*
[12]*Center for Nuclear Study, Graduate School of Science, University of Tokyo, 7-3-1 Hongo, Bunkyo, Tokyo 113-0033, Japan*
[13]*University of Colorado, Boulder, Colorado 80309, USA*
[14]*Columbia University, New York, New York 10027 and Nevis Laboratories, Irvington, New York 10533, USA*
[15]*Czech Technical University, Zikova 4, 166 36 Prague 6, Czech Republic*
[16]*Dapnia, CEA Saclay, F-91191, Gif-sur-Yvette, France*
[17]*ELTE, Eötvös Loránd University, H-1117 Budapest, Pázmány P. s. 1/A, Hungary*
[18]*Ewha Womans University, Seoul 120-750, Korea*
[19]*Florida Institute of Technology, Melbourne, Florida 32901, USA*
[20]*Florida State University, Tallahassee, Florida 32306, USA*
[21]*Georgia State University, Atlanta, Georgia 30303, USA*
[22]*Hiroshima University, Kagamiyama, Higashi-Hiroshima 739-8526, Japan*
[23]*Department of Physics and Astronomy, Howard University, Washington, DC 20059, USA*
[24]*IHEP Protvino, State Research Center of Russian Federation, Institute for High Energy Physics, Protvino, 142281, Russia*
[25]*University of Illinois at Urbana-Champaign, Urbana, Illinois 61801, USA*
[26]*Institute for Nuclear Research of the Russian Academy of Sciences, prospekt 60-letiya Oktyabrya 7a, Moscow 117312, Russia*
[27]*Institute of Physics, Academy of Sciences of the Czech Republic, Na Slovance 2, 182 21 Prague 8, Czech Republic*
[28]*Iowa State University, Ames, Iowa 50011, USA*
[29]*Advanced Science Research Center, Japan Atomic Energy Agency, 2-4 Shirakata Shirane, Tokai-mura, Naka-gun, Ibaraki-ken 319-1195, Japan*
[30]*Helsinki Institute of Physics and University of Jyväskylä, P.O.Box 35, FI-40014 Jyväskylä, Finland*
[31]*Károly Róberts University College, H-3200, Mátrai út 36 Gyöngyös, Hungary*
[32]*KEK, High Energy Accelerator Research Organization, Tsukuba, Ibaraki 305-0801, Japan*
[33]*Korea University, Seoul, 136-701, Korea*
[34]*National Research Center "Kurchatov Institute," Moscow, 123098 Russia*
[35]*Kyoto University, Kyoto 606-8502, Japan*
[36]*Laboratoire Leprince-Ringuet, Ecole Polytechnique, CNRS-IN2P3, Route de Saclay, F-91128, Palaiseau, France*
[37]*Physics Department, Lahore University of Management Sciences, Lahore 54792, Pakistan*
[38]*Lawrence Livermore National Laboratory, Livermore, California 94550, USA*
[39]*Los Alamos National Laboratory, Los Alamos, New Mexico 87545, USA*

[40]LPC, Université Blaise Pascal, CNRS-IN2P3, Clermont-Fd, 63177 Aubiere Cedex, France

[41]Department of Physics, Lund University, Box 118, SE-221 00 Lund, Sweden

[42]University of Maryland, College Park, Maryland 20742, USA

[43]Department of Physics, University of Massachusetts, Amherst, Massachusetts 01003-9337, USA

[44]Department of Physics, University of Michigan, Ann Arbor, Michigan 48109-1040, USA

[45]Institut für Kernphysik, University of Muenster, D-48149 Muenster, Germany

[46]Muhlenberg College, Allentown, Pennsylvania 18104-5586, USA

[47]Myongji University, Yongin, Kyonggido 449-728, Korea

[48]Nagasaki Institute of Applied Science, Nagasaki-shi, Nagasaki 851-0193, Japan

[49]Nara Women's University, Kita-uoya Nishi-machi Nara 630-8506, Japan

[50]National Research Nuclear University, MEPhI, Moscow Engineering Physics Institute, Moscow, 115409, Russia

[51]University of New Mexico, Albuquerque, New Mexico 87131, USA

[52]New Mexico State University, Las Cruces, New Mexico 88003, USA

[53]Department of Physics and Astronomy, Ohio University, Athens, Ohio 45701, USA

[54]Oak Ridge National Laboratory, Oak Ridge, Tennessee 37831, USA

[55]IPN-Orsay, Univ. Paris-Sud, CNRS/IN2P3, Université Paris-Saclay, BP1, F-91406, Orsay, France

[56]Peking University, Beijing 100871, People's Republic of China

[57]PNPI, Petersburg Nuclear Physics Institute, Gatchina, Leningrad region, 188300, Russia

[58]RIKEN Nishina Center for Accelerator-Based Science, Wako, Saitama 351-0198, Japan

[59]RIKEN BNL Research Center, Brookhaven National Laboratory, Upton, New York 11973-5000, USA

[60]Physics Department, Rikkyo University, 3-34-1 Nishi-Ikebukuro, Toshima, Tokyo 171-8501, Japan

[61]Saint Petersburg State Polytechnic University, St. Petersburg, 195251 Russia

[62]Universidade de São Paulo, Instituto de Física, Caixa Postal 66318, São Paulo CEP05315-970, Brazil

[63]Department of Physics and Astronomy, Seoul National University, Seoul 151-742, Korea

[64]Chemistry Department, Stony Brook University, SUNY, Stony Brook, New York 11794-3400, USA

[65]Department of Physics and Astronomy, Stony Brook University, SUNY, Stony Brook, New York 11794-3800, USA

[66]University of Tennessee, Knoxville, Tennessee 37996, USA

[67]Department of Physics, Tokyo Institute of Technology, Oh-okayama, Meguro, Tokyo 152-8551, Japan

[68]Center for Integrated Research in Fundamental Science and Engineering, University of Tsukuba, Tsukuba, Ibaraki 305, Japan

[69]Vanderbilt University, Nashville, Tennessee 37235, USA

[70]Waseda University, Advanced Research Institute for Science and Engineering, 17 Kikui-cho, Shinjuku-ku, Tokyo 162-0044, Japan

[71]Weizmann Institute, Rehovot 76100, Israel

[72]Institute for Particle and Nuclear Physics, Wigner Research Centre for Physics, Hungarian Academy of Sciences
(Wigner RCP, RMKI) H-1525 Budapest 114, POBox 49, Budapest, Hungary

[73]Yonsei University, IPAP, Seoul 120-749, Korea

[74]University of Zagreb, Faculty of Science, Department of Physics, Bijenička 32, HR-10002 Zagreb, Croatia

Jet production rates are measured in $p + p$ and $d + Au$ collisions at $\sqrt{s_{NN}} = 200$ GeV recorded in 2008 with the PHENIX detector at the Relativistic Heavy Ion Collider. Jets are reconstructed using the $R = 0.3$ anti-k_t algorithm from energy deposits in the electromagnetic calorimeter and charged tracks in multiwire proportional chambers, and the jet transverse momentum (p_T) spectra are corrected for the detector response. Spectra are reported for jets with $12 < p_T < 50$ GeV/c, within a pseudorapidity acceptance of $|\eta| < 0.3$. The nuclear-modification factor (R_{dAu}) values for 0%–100% $d + Au$ events are found to be consistent with unity, constraining the role of initial state effects on jet production. However, the centrality-selected R_{dAu} values and central-to-peripheral ratios (R_{CP}) show large, p_T-dependent deviations from unity, challenging the conventional models that relate hard-process rates and soft-particle production in collisions involving nuclei.

Jet cross-section measurements in $d + Au$ collisions at the Relativistic Heavy Ion Collider (RHIC) are crucial for benchmarking the effects of the so-called cold-nuclear-matter environment, where jet production rates are expected to be sensitive to the modification of the nuclear parton densities [1] or to the energy loss of fast partons in the nucleus [2–4]. Recent observations of collective behavior in small

collision systems at the Large Hadron Collider (LHC) and RHIC [5–8] suggest that jet quenching in a possibly formed quark-gluon plasma [9] may play a role as well. Measurements of jet production as a function of centrality, an experimental proxy for the impact parameter of the deuteron with respect to the nucleus, are particularly important. They may reveal the impact parameter dependence of the nuclear

parton densities [10], of nonlinear quantum chromodynamics (QCD) effects at very high parton densities [11,12], or of energy loss. More generally, they test the applicability of geometric models that describe how soft observables and hard process rates in heavy ion collisions are related [13]. At RHIC energies, jet spectra have previously been reported only in $p + p$ collisions [14,15].

Modifications to jet production rates from the vacuum expectation are quantified through the nuclear-modification factor $R_{dAu} \equiv (dN^{cent}/dp_T)/(T_{dAu}^{cent} d\sigma/dp_T)$, where the numerator is the per-event jet yield as a function of transverse momentum (p_T) in a given class of $d + Au$ collisions ("cent"), and the denominator is the jet production cross section in $p + p$ collisions scaled by the corresponding mean value of the nuclear-overlap function T_{dAu}. Because T_{dAu} cannot be directly determined experimentally, it is typically calculated within a Glauber model of relativistic nuclear collisions. R_{dAu} values of unity mean that the jet rate in $d + Au$ collisions is consistent with that in $p + p$ collisions after correcting for the larger degree of partonic overlap. The double ratio of the R_{dAu} in central (large T_{dAu}) events to that in peripheral (small T_{dAu}) events, R_{CP}, quantifies the relative modification between $d + Au$ event classes.

Previous measurements of hadron production at midrapidity in $d + Au$ collisions [16,17] found that R_{dAu} is consistent with unity at $p_T = 5$–10 GeV/c for all centralities, implying that hard-process yields scale with the overlap of the incoming partons and constraining the role of nuclear effects. The data further suggested that R_{dAu} for $p_T > 10$ GeV/c deviates from unity [16], but with small statistical significance. Recent measurements of $p_T \gtrsim 100$ GeV/c jet and dijet production in $p + Pb$ collisions at the LHC showed a large, unexpected sensitivity to the collision centrality [18,19]. A number of novel explanations [20–22] have been proposed for these effects, which are generally expected to persist to RHIC energies, but at large p_T where previous measurements have lacked statistical precision. This Letter presents the centrality dependence of jet production in an asymmetric collision system over a kinematic range previously not measured at RHIC.

Jets were measured in one of the PHENIX central spectrometers (the "East" arm) [23] during data taking in 2008. The spectrometer provides a pseudorapidity aperture of $|\eta| < 0.35$, $\pi/2$ coverage in azimuth, and is situated outside a 0.9 T axial magnetic field. Charged-particle tracks are measured by a set of multiwire proportional chambers, including an inner drift chamber and multiple outer pad chambers that together provide a resolution of $\sigma_p/p = 0.7\% \oplus 1\% p$ where p is in GeV/c. Energy deposits from neutral particles are measured by the finely segmented electromagnetic calorimeter, composed of two lead-glass Čerenkov and two lead-scintillator sectors, which have a resolution determined by beam tests [24] to be $\sigma_E/E = 5.9\%/\sqrt{E} \oplus 0.8\%$ and $8.1\%/\sqrt{E} \oplus 2.1\%$, respectively,

where E is in GeV. Calibration was performed through the reconstruction of neutral pion decays. The calorimeter further provides a trigger signal initiated by the presence of at least 1.6 or 2.1 GeV of energy deposited in one of the groups of overlapping 4×4 towers in the lead-glass or lead-scintillator modules, respectively. In addition to the spectrometer, a pair of beam-beam counter detectors situated along the beam line at $3.0 < |\eta| < 3.9$ provide the minimum-bias trigger signal and reconstruct the z position of the primary vertex.

The analyzed $p + p$ and $d + Au$ data sets were carefully chosen, and the single central arm was used, to ensure a large, stable and uniform acceptance for jets, and corresponded to 2.0 pb^{-1} and 23 nb^{-1} (equivalent to an integrated nucleon-nucleon luminosity of 9.1 pb^{-1}), respectively. The centrality of $d + Au$ collisions was characterized using the total charge deposited in the Au-going beam-beam counter. A Glauber Monte Carlo [13,25] description of $d + Au$ collisions was used, along with the hypothesis that this charge increased linearly with the number of nucleon-nucleon collisions [26], to determine the fraction of $d + Au$ collisions accepted by the minimum-bias trigger, $88\% \pm 4\%$, and to estimate the mean value of the nuclear-overlap function T_{dAu}^{cent} for 0%–100% centrality events, as well as those defined by the centrality intervals ("cent") of 0%–20%, 20%–40%, 40%–60%, and 60%–88%. The relationship between the Au-going charge and the collision geometry has been validated through, for example, an analysis of forward neutron production in $d + Au$ collisions, and analyses of $p + p$ collisions indicate that it should hold for events that produce $p_T = 20$ GeV hadrons [26].

In this analysis, the final-state jet definition is specified by applying the anti-k_t algorithm [27,28] with radius parameter $R = 0.3$ to electromagnetic clusters (in the calorimeter) and charged-particle tracks (in the drift and pad chambers), each with a minimum p_T of 0.4 GeV/c. The anti-k_t algorithm clusters outward from the hard core of the jets, reducing the sensitivity to detector edges. A detailed set of criteria designed to select charged particles with a well-measured momentum while ensuring a large and uniform acceptance were applied to candidate reconstructed tracks. Clusters consistent with arising from the same particle as a reconstructed track were rejected to avoid double counting jet constituent energy. Jets which are dominated by reconstructed tracks with a large, erroneously measured p_T [29] were rejected by requiring at least three constituent particles and by requiring at least one quarter of the momentum to arise from clusters. To ensure that the core of the jet is fully contained within the detector, the jet axis was required to be separated from the edge of the acceptance by 0.05 units in pseudorapidity and azimuth.

Detector-level jets, defined as those passing the above criteria, were used to form a transverse momentum spectrum (p_T^{rec}) in each event class. The contribution of the small underlying event background was not subtracted on a

jet-by-jet basis, but was corrected for in the unfolding procedure described below. Jets were selected from the triggered data if a jet constituent fell into the same region of the calorimeter that provided the trigger signal. The trigger efficiency was estimated for each event class by checking this condition as a function of p_T^{rec} in minimum-bias events. The p_T^{rec}-level spectra were corrected for this efficiency, which rose monotonically with p_T^{rec} and was approximately 70% (98%) at 10 GeV/c (25 GeV/c).

Monte Carlo simulations were used to determine the response of the detector to jets and to correct the measured spectra. In simulation, jets are defined by applying the anti-k_t algorithm to long-lived primary particles, resulting in jets with a particle-level transverse momentum (p_T). The PYTHIA 6.4 event generator [30] with the D6T tune [31] and CTEQL1 parton distribution function set [32] was used to generate hard scattering $p + p$ events with a jet within the acceptance of the East arm. Six separate samples with exclusive selections on the hard-scattering momentum transfer in PYTHIA, consisting of 10^5 events each, were weighted according to their partial cross section and combined to form a p_T spectrum from 8 to 80 GeV/c. The response of the detector was simulated with GEANT3 [33] and the resulting events were analyzed identically to the data. To understand the effects of the underlying event in $d + $Au collisions, jet reconstruction was also performed on the simulated events after they were embedded into minimum-bias $d + $Au data events of each centrality. In each event class, particle-level jets were matched with detector-level jets and the correspondence between the true p_T and the measured p_T^{rec} was collected into a response matrix $\mathcal{R}(p_T, p_T^{\text{rec}})$.

The reconstruction and selection efficiency, $\epsilon(p_T)$, for particle-level jets within $|\eta| < 0.3$ rose with p_T and was $\approx$35% (50%) at 10 GeV/c (25 GeV/c) in $p + p$ collisions. The inefficiency was dominated by the minimum requirement on the calorimetric fraction of the jet momentum. For a given selection on the particle-level jet p_T, the mean value of the p_T^{rec}/p_T distribution $\approx$0.65–0.70 resulted from missing neutral hadronic energy and tracking inefficiency. The width of this distribution was $\approx$20%–25%, rose slightly with p_T, and was driven by jet-by-jet fluctuations in the neutral hadronic momentum fraction and not by the resolution on the constituent momenta. In the $d + $Au event classes, the impact of the underlying event on the response decreased systematically with increasing jet p_T. For $p_T = 20$ GeV/c jets in 0%–20% centrality $d + $Au events, the underlying event background increased the efficiency by 2%, the average p_T^{rec} by 0.1–0.2 GeV/c, and the p_T^{rec} resolution by 1%, relative to that in $p + p$ events.

The p_T^{rec}-level spectra were corrected for the detector response and the presence of the underlying event in $d + $Au collisions through the singular-value-decomposition unfolding method [34,35]. For an observed spectrum dN/dp_T^{rec}, this method inverts the equation $dN/dp_T^{\text{rec}} = \mathcal{R}dN/dp_T$ by expressing dN/dp_T as a linear combination

of the left singular vectors of $\mathcal{R}$, with coefficients determined by dN/dp_T^{rec}. This inversion is regularized by keeping the contribution only from the k vectors with the largest singular values. The contribution from the remaining vectors is truncated to ensure that dN/dp_T is unaffected by statistical fluctuations.

Following standard techniques [34], k was fixed at 5, and the results were validated by comparing dN/dp_T, propagated through $\mathcal{R}$, to dN/dp_T^{rec}, and by examining the curvature of dN/dp_T with respect to the simulated p_T spectrum used to populate $\mathcal{R}$. The iterative Bayesian method [36] gave consistent results. The statistical uncertainties on dN/dp_T were evaluated by resampling dN/dp_T^{rec} according to its uncertainties and observing the changes in dN/dp_T. Finally, the dN/dp_T spectra were corrected for the reconstruction efficiency $\epsilon(p_T)$. At low p_T in 0%–20% events, the $R_{d\text{Au}}$ after unfolding was lower than the detector-level $R_{d\text{Au}}$ by $\approx$20%, while the two are comparable at high p_T or in peripheral events.

The $p + p$ differential cross section was constructed [16] via $2\pi\sigma^{pp}N^{\text{jet}}(p_T)/\epsilon^{pp}N^{\text{evt}}\epsilon(p_T)\Delta p_T\Delta\eta\Delta\phi$, where $\sigma^{pp} = 23.0 \pm 2.2$ mb is the minimum-bias cross section, $\epsilon^{pp} = 0.79 \pm 0.02$ is the fraction of jet events meeting the minimum-bias condition, and $2\pi/\Delta p_T\Delta\eta\Delta\phi$ are phase-space factors. Figure 1 shows the $d + $Au yields and the $p + p$ cross section, which compares well with a perturbative QCD calculation [37,38].

The measured spectra and nuclear-modification factors are subject to systematic uncertainties from a variety of sources. For most sources, the effects on the results were determined by modifying the simulation sample, the event or jet-selection criteria, or the unfolding procedure itself,
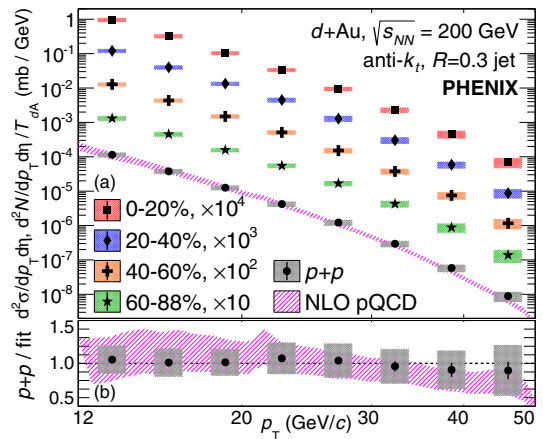

FIG. 1. (a) Measured anti-k_t, $R = 0.3$ jet yields in $d + $Au collisions, and the measured and calculated jet cross section in $p + p$ collisions, with the data series offset by multiplicative factors. Total systematic uncertainties, including overall normalization uncertainties, and statistical uncertainties are shown as shaded bands and vertical bars, respectively. (b) The $p + p$ data and perturbative QCD calculation [37,38] are divided by a fit to the data.

and repeating the analysis. The variations were applied simultaneously in the analyses of the $d + Au$ and $p + p$ spectra to allow for their full or partial cancellation in the R_{dAu} and R_{CP} quantities, with the exception of the variation of k, described below.

The impact of uncertainties on the detector energy scales was determined by varying the momenta of the reconstructed tracks and clusters in simulation. The cluster energies were varied by 3%. The track momenta were varied by a track p_T-dependent amount, which was 2% for $p_T \leq 10$ GeV/c and increased linearly to 4% for $p_T = 30$ GeV/c. The sensitivity of the results to the jet selection was evaluated by varying the maximum and minimum requirement on the calorimetric content of the jet, and by raising the required number of jet constituents. The uncertainty in the jet acceptance was evaluated by doubling the fiducial distance between jets and the edges of the detector, and by restricting the vertex z position to a narrower range. The uncertainties associated with the unfolding procedure were evaluated by changing the power law index of the simulated p_T spectrum by ± 1, and by increasing and decreasing the value of k. Because they are statistical in nature, the effects on the spectra from varying k were treated as uncorrelated between the event classes. The sensitivity to the underlying physics model was evaluated by performing the corrections with a sample of PYTHIA events analogous to the nominal one but generated with TUNE A [39] and the CTEQ5L [40] set. A 2% uncertainty, uncorrelated between event classes, was assigned to the spectra below 25 GeV/c to cover possible defects in modeling the trigger efficiency.

For each observable, the magnitudes of the resulting changes were added in quadrature to obtain a total systematic uncertainty. The total uncertainty on the spectra increased from 12% at $p_T = 12$ GeV/c to 30% or higher at $p_T = 50$ GeV/c and was dominated at all p_T by the energy scale. Because the reconstruction procedure in $d + Au$ and $p + p$ collisions was identical, and the performance, corrections, and resulting spectra are very similar, the effects of the variations on R_{dAu} and R_{CP} canceled to a large degree. The uncertainties on this quantity ranged from 4% at $p_T = 12$ GeV/c (with no single source dominating) to 15% or higher (dominated by unfolding and physics model) at $p_T = 50$ GeV/c.

Additional normalization uncertainties on the $p + p$ cross section of 10% arose from the uncertainty on $\sigma^{pp}/\epsilon^{pp}$. Uncertainties in the determination of T_{dAu} contributed to the R_{dAu} and R_{CP}, such that the total uncertainty on these ranged from 3% to 13%.

Figure 2 summarizes the measured R_{dAu} and R_{CP} quantities. The 0%–100% R_{dAu} is consistent with unity at all p_T values and is p_T independent within uncertainties. The data are consistent with a next-to-leading order calculation [41–44] incorporating the EPS09 [1] nuclear-parton-density set, suggesting that nuclear effects are small
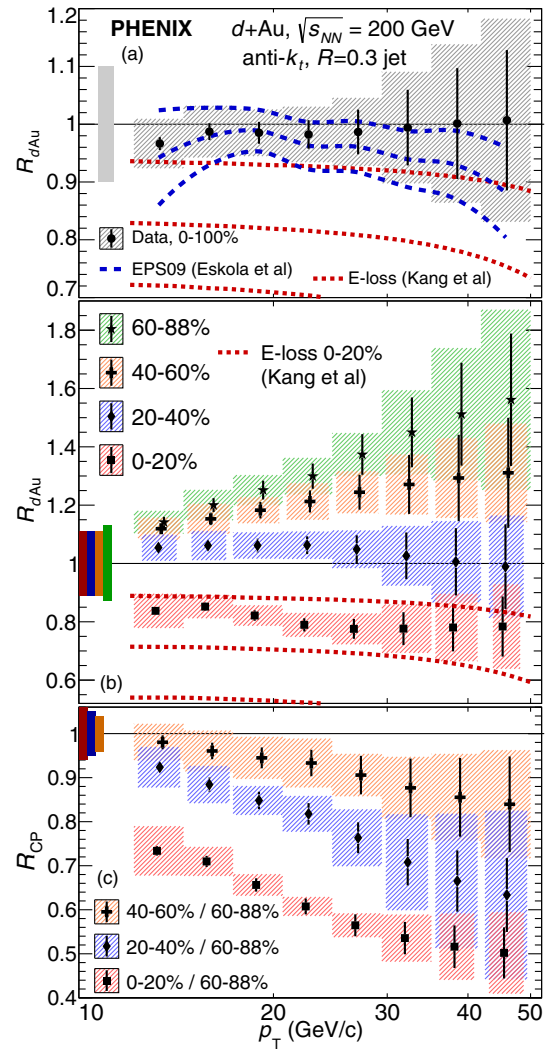

FIG. 2. R_{dAu} for (a) 0%–100% and (b) centrality-selected collisions, and (c) R_{CP}, as a function of p_T. Systematic, statistical, and normalization uncertainties are shown as shaded bands, vertical bars, and the leftmost bands centered at 1, respectively. When error bands overlap vertically, their horizontal widths have been adjusted so that both are visible. Dashed lines show the uncertainty range of calculations incorporating nuclear parton densities [1] and energy loss [4].

at high Q^2 in the nuclear Bjorken-x range ≈ 0.1–0.5. When compared to calculations over a range of energy loss rates in the cold nucleus [4], the data favor only small momentum transfers between the hard-scattered parton and nuclear material, providing constraints on initial-state, or any additional final-state, energy loss.

In contrast, the centrality-dependent R_{dAu} values strongly deviate from unity, manifesting as a suppression ($R_{dAu} < 1$) and enhancement ($R_{dAu} > 1$) in central and peripheral collisions, respectively, which increase in magnitude with p_T. Accordingly, the R_{CP} is < 1 in most selections and decreases systematically with p_T and in more central events. While the suppressed R_{dAu} in 0%–20% events is consistent with a calculation incorporating

modest energy loss, an enhancement in 40%–88% events, which coincidentally cancels with the suppression to produce an unmodified minimum bias rate, is challenging to understand as a distinct physics effect.

If jet production is unmodified but a physics bias enters into the centrality classification, this could naturally explain the R_{dAu} results. In fact, measurements of centrality-dependent yields are understood to be biased by the increased multiplicity in hard-scattering nucleon-nucleon events [26,45–47], which generally increases (decreases) the yield in central (peripheral) collisions. The results have been corrected for this bias following Ref. [26], thus slightly increasing the magnitude of the modifications. On the other hand, if the charged particle multiplicity several units of rapidity away in the Au-going direction were suppressed instead of enhanced in $p_T > 12$ GeV/c jet events, this would reverse the sign of the correction and could result in the observed modifications. The jet p_T dependence of this correlation has been studied in $p + p$ data and in HIJING [48], where it is well reproduced. The decreased multiplicity results in modest changes ($< 5\%$) in the correction factors for events with $p_T = 20$ GeV/c hadrons [26], a much smaller effect than what is needed to describe the R_{dAu} data. Thus, no feature of elemental $p + p$ collisions can explain the data alone, indicating the relevance of the large nucleus and the need for successful models to describe the correlation between soft and hard processes in $p + p$ and $d + $ Au.

At midrapidity, jet production in $p + $ Pb collisions at the LHC [18] follows a similar modification pattern in the Bjorken-x range, $x_p \sim x_{Pb} \gtrsim 0.1$. However, the R_{pPb} in those results scales with proton x, suggesting a scenario in which the modifications arise from a novel feature of the proton wave function at large x [20–22]. For example, if high-x deuteron configurations have a weaker than average interaction strength and strike fewer nucleons in the Au nucleus [21], this would result in the unmodified, suppressed, and enhanced R_{dAu} in minimum-bias, central, and peripheral events, respectively. If so, the observed centrality dependence of forward hadron production [49–52] in $d + $ Au collisions may arise from the same mechanism as the results presented here, because both are kinematically associated with the scattering of a large-x parton in the deuteron. Finally, using an alternate estimate of T_{dAu} provided by applying the Glauber-Gribov color fluctuation model [53,54] to the data would increase the deviation of R_{dAu} in the most central and peripheral events from unity by 10% and 5%, respectively.

This Letter presents the first measurement of high-p_T jet production in $d + $ Au collisions at RHIC. The jet rate in inclusive collisions is broadly consistent with expectations, providing constraints in a new kinematic regime on modifications to the parton densities in nuclei and on the energy loss of fast partons in the nuclear medium. When compared to the expectation from geometric considerations, the rates in centrality-selected events strongly deviate from unity, featuring suppression and enhancement patterns in central and peripheral events, respectively. These deviations grow with increasing p_T, but cancel in the overall jet rate, and challenge the conventional pictures of how hard-process rates and soft-particle production are related in collisions involving nuclei.

––––––––––––––

*Deceased.

†PHENIX Spokesperson.
 morrison@bnl.gov

‡PHENIX Spokesperson.
 jamie.nagle@colorado.edu

[1] K. J. Eskola, H. Paukkunen, and C. A. Salgado, EPS09: A new generation of NLO and LO nuclear parton distribution functions, J. High Energy Phys. 04 (2009) 065.

[2] I. Vitev, Non-Abelian energy loss in cold nuclear matter, Phys. Rev. C **75**, 064906 (2007).

[3] Z.-B. Kang, I. Vitev, and H. Xing, Nuclear modification of high transverse momentum particle production in $p + A$ collisions at RHIC and LHC, Phys. Lett. B **718**, 482 (2012).

[4] Z.-B. Kang, I. Vitev, and H. Xing, Effects of cold-nuclear-matter energy loss on inclusive jet production in $p + A$ collisions at energies available at the BNL Relativistic Heavy Ion Collider and the CERN Large Hadron Collider, Phys. Rev. C **92**, 054911 (2015).

[5] S. Chatrchyan *et al.* (CMS Collaboration), Observation of long-range near-side angular correlations in proton-lead collisions at the LHC, Phys. Lett. B **718**, 795 (2013).

[6] Georges Aad *et al.* (ATLAS Collaboration), Observation of Associated Near-Side and Away-Side Long-Range Correlations in $\sqrt{s_{NN}} = 5.02$ TeV Proton-Lead Collisions with the ATLAS Detector, Phys. Rev. Lett. **110**, 182302 (2013).

[7] Betty Abelev *et al.* (ALICE Collaboration), Long-range angular correlations on the near and away side in pPb collisions at $\sqrt{s_{NN}} = 5.02$ TeV, Phys. Lett. B **719**, 29 (2013).

[8] A. Adare *et al.* (PHENIX Collaboration), Quadrupole Anisotropy in Dihadron Azimuthal Correlations in Central $d + Au$ Collisions at $\sqrt{s_{NN}} = 200$ GeV, Phys. Rev. Lett. **111**, 212301 (2013).

[9] X. Zhang and J. Liao, Jet quenching and its azimuthal anisotropy in AA and possibly high multiplicity pA and dA collisions, arXiv:1311.5463.

[10] I. Helenius, K. J. Eskola, H. Honkanen, and C. A. Salgado, Impact-parameter dependent nuclear parton distribution functions: EPS09s and EKS98s and their applications in nuclear hard processes, J. High Energy Phys. 07 (2012) 073.

[11] J. L. Albacete, A. Dumitru, Hirotsugu Fujii, and Y. Nara, CGC predictions for $p + Pb$ collisions at the LHC, Nucl. Phys. **A897**, 1 (2013).

[12] A. H. Rezaeian, CGC predictions for $p + A$ collisions at the LHC and signature of QCD saturation, Phys. Lett. B **718**, 1058 (2013).

[13] M. L. Miller, K. Reygers, S. J. Sanders, and P. Steinberg, Glauber modeling in high energy nuclear collisions, Annu. Rev. Nucl. Part. Sci. **57**, 205 (2007).

[14] B. I. Abelev *et al.* (STAR Collaboration), Longitudinal double-spin asymmetry and cross section for inclusive jet production in polarized proton collisions at $\sqrt{s} = 200$ GeV, Phys. Rev. Lett. **97**, 252001 (2006).

[15] L. C. Bland *et al.* (AnDY Collaboration), Cross sections and transverse single-spin asymmetries in forward jet production from proton collisions at $\sqrt{s} = 500$ GeV, Phys. Lett. B **750**, 660 (2015).

[16] S. S. Adler *et al.* (PHENIX Collaboration), Centrality Dependence of π^0 and η Production at Large Transverse Momentum in $\sqrt{s_{NN}} = 200$ GeV $d + Au$ Collisions, Phys. Rev. Lett. **98**, 172302 (2007).

[17] B. I. Abelev *et al.* (STAR Collaboration), Inclusive π^0, η, and direct photon production at high transverse momentum in $p + p$ and $d + Au$ collisions at $\sqrt{s_{NN}} = 200$ GeV, Phys. Rev. C **81**, 064904 (2010).

[18] G. Aad *et al.* (ATLAS Collaboration), Centrality and rapidity dependence of inclusive jet production in $\sqrt{s_{NN}} = 5.02$ TeV proton-lead collisions with the ATLAS detector, Phys. Lett. B **748**, 392 (2015).

[19] S. Chatrchyan *et al.* (CMS Collaboration), Studies of dijet transverse momentum balance and pseudorapidity distributions in pPb collisions at $\sqrt{s_{NN}} = 5.02$ TeV, Eur. Phys. J. C **74**, 2951 (2014).

[20] A. Bzdak, V. Skokov, and S. Bathe, Centrality dependence of high energy jets in $p + Pb$ collisions at the LHC, arXiv:1408.3156.

[21] M. Alvioli, B. A. Cole, L. Frankfurt, D. V. Perepelitsa, and M. Strikman, Evidence for x-dependent proton color fluctuations in pA collisions at the CERN Large Hadron Collider, Phys. Rev. C **93**, 011902 (2016).

[22] N. Armesto, D. C. Gülhan, and J. G. Milhano, Kinematic bias on centrality selection of jet events in pPb collisions at the LHC, Phys. Lett. B **747**, 441 (2015).

[23] K. Adcox *et al.* (PHENIX Collaboration), PHENIX detector overview, Nucl. Instrum. Methods Phys. Res., Sect. A **499**, 469 (2003).

[24] G. David *et al.* (PHENIX Collaboration), The PHENIX lead-scintillator electromagnetic calorimeter: Test beam and construction experience, Nuclear Science and Medical Imaging, *Proceedings, Symposium and Conference, NSS/ MIC, Albuquerque, USA, November* (1997); [IEEE Trans. Nucl. Sci. **45**, 692 (1998)].

[25] B. Alver, M. Baker, C. Loizides, and P. Steinberg, The PHOBOS Glauber Monte Carlo, arXiv:0805.4411.

[26] A. Adare *et al.* (PHENIX Collaboration), Centrality categorization for $R_{p(d)+A}$ in high-energy collisions, Phys. Rev. C **90**, 034902 (2014).

[27] M. Cacciari, G. P. Salam, and G. Soyez, The anti-k_t jet clustering algorithm, J. High Energy Phys. 04 (2008) 063.

[28] M. Cacciari, G. P. Salam, and G. Soyez, FastJet User Manual, Eur. Phys. J. C **72**, 1896 (2012).

[29] K. Adcox *et al.* (PHENIX Collaboration), Centrality dependence of the high p_T charged hadron suppression in Au + Au collisions at $\sqrt{s_{NN}} = 130$ GeV, Phys. Lett. B **561**, 82 (2003).

[30] T. Sjostrand, S. Mrenna, and P. Z. Skands, PYTHIA 6.4 Phys. and Manual, J. High Energy Phys. 05 (2006) 026.

[31] M. G. Albrow *et al.* (TeV4LHC QCD Working Group), Tevatron-for-LHC Report of the QCD Working Group, arXiv:hep-ph/0610012.

[32] J. Pumplin, D. R. Stump, J. Huston, H. L. Lai, P. M. Nadolsky, and W. K. Tung, New generation of parton distributions with uncertainties from global QCD analysis, J. High Energy Phys. 07 (2002) 012.

[33] R. Brun, F. Bruyant, M. Maire, A. C. McPherson, and P. Zanarini, Geant Users Guide, 3.15, CERN program library, cern-dd-ee-84-1 (1987).

[34] A. Hocker and V. Kartvelishvili, SVD approach to data unfolding, Nucl. Instrum. Methods Phys. Res., Sect. A **372**, 469 (1996).

[35] T. Adye, Unfolding algorithms and tests using RooUnfold, in *Proceedings of the PHYSTAT 2011 Workshop, CERN, Geneva, Switzerland, January 2011, CERN-2011-006* (CERN, Geneva, 2011), p. 313.

[36] G. D'Agostini, A Multidimensional unfolding method based on Bayes' theorem, Nucl. Instrum. Methods Phys. Res., Sect. A **362**, 487 (1995).

[37] Z. Nagy, Next-to-leading order calculation of three jet observables in hadron hadron collision, Phys. Rev. D **68**, 094002 (2003).

[38] R. D. Ball, L. Del Debbio, S. Forte, A. Guffanti, J. I. Latorre, J. Rojo, and M. Ubiali, A first unbiased global NLO determination of parton distributions and their uncertainties, Nucl. Phys. **B838**, 136 (2010).

[39] R. D. Field (CDF Collaboration), The Underlying event in hard scattering processes, in *Proceedings of APS/DPF/DPB Summer Study on the Future of Particle Phys. (Snowmass 2001), Snowmass, Colorado, 30 Jun–21 Jul 2001*, eConf C010630 (2001) P501.

[40] H. L. Lai, J. Huston, S. Kuhlmann, J. Morfin, F. I. Olness, J. F. Owens, J. Pumplin, and W. K. Tung (CTEQ Collaboration), Global QCD analysis of parton structure of the nucleon: CTEQ5 parton distributions, Eur. Phys. J. C **12**, 375 (2000).

[41] Calculation performed by N. Armesto (private communication).

[42] S. Frixione, Z. Kunszt, and A. Signer, Three jet cross-sections to next-to-leading order, Nucl. Phys. **B467**, 399 (1996).

[43] S. Frixione, A General approach to jet cross-sections in QCD, Nucl. Phys. **B507**, 295 (1997).

[44] S. Frixione and G. Ridolfi, Jet photoproduction at HERA, Nucl. Phys. **B507**, 315 (1997).

[45] S. S. Adler *et al.* (PHENIX Collaboration), Nuclear effects on hadron production in $d + \text{Au}$ and $p + p$ collisions at $\sqrt{s_{NN}} = 200$ GeV, Phys. Rev. C **74**, 024904 (2006).

[46] D. V. Perepelitsa and P. A. Steinberg, Calculation of centrality bias factors in $p + A$ collisions based on a positive correlation of hard process yields with underlying event activity, arXiv:1412.0976.

[47] J. Adam *et al.* (ALICE Collaboration), Centrality dependence of particle production in $p\text{Pb}$ collisions at $\sqrt{s_{NN}} = 5.02$ TeV, Phys. Rev. C **91**, 064905 (2015).

[48] M. Gyulassy and X.-N. Wang, HIJING 1.0: A Monte Carlo program for parton and particle production in high-energy hadronic and nuclear collisions, Comput. Phys. Commun. **83**, 307 (1994).

[49] I. Arsene *et al.* (BRAHMS Collaboration), On the Evolution of the Nuclear Modification Factors with Rapidity and Centrality in $d + \text{Au}$ Collisions at $\sqrt{s_{NN}} = 200$ GeV, Phys. Rev. Lett. **93**, 242303 (2004).

[50] S. S. Adler *et al.* (PHENIX Collaboration), Nuclear Modification Factors for Hadrons at Forward and Backward Rapidities in Deuteron-Gold Collisions at $\sqrt{s_{NN}} = 200$ GeV, Phys. Rev. Lett. **94**, 082302 (2005).

[51] B. I. Abelev *et al.* (STAR Collaboration), Charged particle distributions and nuclear modification at high rapidities in $d + \text{Au}$ collisions at $\sqrt{s_{NN}} = 200$ GeV, arXiv:nucl-ex/0703016.

[52] A. Adare *et al.* (PHENIX Collaboration), Suppression of Back-to-Back Hadron Pairs at Forward Rapidity in $d + \text{Au}$ Collisions at $\sqrt{s_{NN}} = 200$ GeV, Phys. Rev. Lett. **107**, 172301 (2011).

[53] M. Alvioli and M. Strikman, Color fluctuation effects in proton-nucleus collisions, Phys. Lett. B **722**, 347 (2013).

[54] G. Aad *et al.* (ATLAS Collaboration), Measurement of the centrality dependence of the charged-particle pseudorapidity distribution in proton–lead collisions at $\sqrt{s_{NN}} = 5.02$ TeV with the ATLAS detector, arXiv:1508.00848.